Available online at www.sciencedirect.com

SCIENCE DIRECT®

Journal of Molecular Structure 791 (2006) 18–22

Journal of
MOLECULAR
STRUCTURE

www.elsevier.com/locate/molstruc

Synthesis, crystal structure and photoluminescence of 3-(1-benzotriazole)-4-methyl-coumarin

Tianzhi Yu *, Yuling Zhao, Duowang Fan

Key Laboratory of Opto-Electronic Technology and Intelligent Control (Lanzhou jiaotong University),
Ministry of Education, Lanzhou 730070, China

Received 19 October 2005; received in revised form 29 December 2005; accepted 29 December 2005

Abstract

A novel coumarin derivative containing an electron-transporting moiety (benzotriazole), 3-(1-benzotriazole)-4-methyl-coumarin (BMC), was synthesized from starting substances, i.e. benzotriazole and 2-hydroxyacetophenone. The compound structure was verified by FT-IR, ^{1}H NMR, element analysis and single crystal X-ray crystallography. Crystallographic data reveal a dihedral angle of 108° between the coumarin and benzotriazole rings, which is attributed to the spatial hindrance of a 4-positioned methyl group. The fluorescence and UV–vis absorption of BMC were discussed. The compound exhibits a strong UV emission peak at 385 nm under 360 nm excitation. The molecular structure of BMC was optimized using density functional theory (DFT) at B3LYP/6-31G(d) level, showing that the optimized geometric parameters are in good agreement with experimental data. In addition, the HOMO and LUMO levels of BMC were deduced.

Keywords: Benzotriazole; Coumarin derivative; Crystal structure; Photoluminescence

1. Introduction

Coumarin and its derivatives have been extensively studied due to their commercial applications in several fields. They possess excellent biological activity, such as anticancer and anticoagulant activity [1]. Moreover, this series of compounds has outstanding optical properties, including an extended spectral range, high quantum yields, superior photostability and good solubility in common solvents. So these compounds are widely used as laser dyes [2–3], nonlinear optical chromophores [4], fluorescent whiteners [5], as well as fluorescent labels and probes for physiological measurement [6–9]. Another feature of the coumarin derivatives is that photophysical and spectroscopic properties can be readily modified by the introduction of substituents in the coumarin ring, giving themselves more flexibility to fit well in various applications [10–13]. For example, electron-releasing substituents in 3- or 7- positions not only bring bathochromic shifts of the absorption edge towards long wavelength side, but also enhance band intensity (in absorption and fluorescence). Since 3-(2-benzothiazolyl)-7-diehylaminocoumarin (coumarin 6) is widely used as an emissive dopant in organic light–emitting diodes (OLEDs) based on polymers [14–16] and small molecules [17–18], coumarin derivatives have attracted much attention due to their potential application for OLEDs [19–20].

In this study, we report on the synthesis and photophysical properties of a novel coumarin derivative, 3-(1-benzotriazole)-4-methyl-coumarin (BMC), containing an electron-accepting moiety (benzotriazole). Benzotriazole moiety is chosen as a substituent for the following reasons. First, UV emission of the coumarins was less studied in spite of their well-known fluorescence in visible range; second, the electron-accepting benzotriazole moiety surely benefits the electron-transporting properties of the compounds [21].

2. Experimental

2.1. Materials and methods

2-Hydroxyacetophenone from Acros Organics and 1H-benzotriazole (BTA) from Aldrich were used without further purification. Chloroacetic acid and Phosphorus oxychloride were analytical grade reagents from Tanjin Fuchen

---

* Corresponding author. Tel. +86 931 4956935; fax: +86 931 4956030.
E-mail address: ytz823@hotmail.com (T. Yu).

0022-2860/$ - see front matter © 2006 Elsevier B.V. All rights reserved.
doi:10.1016/j.molstruc.2005.12.022

Chemical Reagent Factory. Phosphorus oxychloride was dried and redistilled before using.

IR spectra (400–4000 cm^{-1}) were measured on a Nicolet Magna FT-IR spectrophotometer. C, H, and N analyses were obtained using an Elemental Vario-EL automatic elemental analysis instrument. 1H NMR spectra were obtained on Unity Varian-500MHz. UV–vis absorption and fluorescence spectra were recorded on a Hitachi UV-3010PC spectrometer and on a Hitachi MPF-4 spectrometer, respectively. Melting points were observed by the capillary tube method.

*2.2. (1-Benzotriazolyl) acetic acid (**1**)*

13.1 g (0.11 mol) of 1H-benzotriazole and 9.45 g (0.1 mol) of chloroacetic acid were dissolved in dry toluene (100 ml), and then the solution was heated to 130 °C and refluxed for 18 h with magnetic stirring. After cooling the solution to room temperature, it was poured into a concentrated aqueous solution of $NaHCO_3$. The water phase was separated and extracted with dichloromethane three times. The aqueous solution was adjusted to a pH of 4 by adding 2N HCl and allowed to sit overnight. After this, the precipitate was filtered and washed successively with distilled water and methanol. The product was dried under reduced pressure and purified with re-crystallization from methanol to yield 10.6 g (60%) of white crystalline solid; m.p. 213–215 °C (Ref.[22]: 214–216 °C).

*2.3. (2-Acetyl) phenol 2-(1-benzotriazolyl) acetate (**2**)*

To a stirred solution of 10 g (0.073 mol) of 2-hydroxyacetophenone and 13.99 g (0.079 mol) of (1-benzotriazolyl) Acetic acid (1) in 100 ml of dry pyridine cooled at 5–10 °C, 6 ml of phosphorus oxychloride was added stepwise. The mixture was stired for 10 h at room temperature. After the reaction was complete, the mixture was allowed to sit overnight. Then the mixture was poured into an aqueous solution of HCl containing fragment ice with vigorous stirring, and a precipitate was produced. The precipitate was filtered and washed successively with diluted aqueous solution of $NaHCO_3$ (10%) and distilled water, respectively. After ethanol recrystallization, filtration and drying in vacuum, 17.35 g (80%) of primrose fine crystals were obtained. m.p. 136–138 °C (Lit. [23]: 137–138 °C).

*2.4. 3-(1-Benzotriazole)-4-methyl-coumarin (**3**)*

6 g (0.02 mol) of (2-acetyl) phenol 2-(1-benzotriazolyl) acetate was dissolved in 50 ml of dry pyridine, then 1.4 g (0.025 mol) of potassium hydroxide was added stepwise and the reaction mixture was stirred vigorously for 5 h at room temperature. The mixture turned brown during the reaction, and the solution became ropy. After completing, the mixture was poured into the aqueous solution of HCl containing fragment ice with vigorous stirring and a yellow precipitate was formed. Then the crude product was filtered and washed with distilled water and purified with recrystallization from ethanol to yield 4.61 g (81.9%) of yellow crystalline solid. m.p. 172–174 °C. Anal. Calc. for $C_{16}H_{11}N_3O_2$ (%): C, 69.31; H, 4.00; N, 15.15. Found: C, 69.16; H, 3.94; N, 15.04. IR (KBr pellet, cm^{-1}): 1718 ($\nu_{C=O}$). 1H NMR (500 MHz, $CDCl_3$, δ, ppm): 2.32m (s, 3H, CH_3), 7.25–8.21 (m, 8H, Ar-H). The compound is soluble in common organic solvents such as chloroform, acetone and tetrahydrofuran.

Table 1
Crystal data and structure refinement for BMC

Empirical formula	$C_{16}H_{11}N_3O_2$
Formula weight	277.28
Temperature (K)	293 (2)
Wavelength (Å)	0.71073
Crystal system	Orthorhombic
Space group	$Pca2_1$
Unit cell dimensions	$a=18.303$ (3) Å, $\alpha=90°$ $b=5.4256$ (8) Å, $\beta=90°$ $c=13.4928$ (19) Å, $\gamma=90°$
Volume ($Å^3$), Z	1339.9 (3), 4
Density (calculated) (g/cm^3)	1.375
Absorption coefficient (mm^{-1})	0.094
F (000)	576
Crystal size (mm)	0.31 × 0.11 × 0.08
θ range for data collected (°)	2.23 to 26.04
Limiting indices	$-20\leq h\leq 22$, $-6\leq k\leq 6$, $-13\leq l\leq 16$
Reflections collected	7024
Independent reflections	2295 ($R_{int}=0.0372$)
Absorption correction	Semi-empirical from equivalents
Max. and min. transmission	0.9922 and 0.9716
Refinement method	Full-matrix least-squares on F^2
Data/restraints/parameters	2295/1/191
Goodness-of-fit on F^2	1.024
Final R indices [$I>2\sigma(I)$]	$R_1=0.0494$, $wR_2=0.1120$
R indices (all data)	$R_1=0.0700$, $wR_2=0.1238$
Largest diff. Peak and hole (e $Å^{-3}$)	0.147 and −0.125

2.5. Crystallography

A suitable single crystal of BMC was obtained from methanol solution. The diffraction data were collected with a Bruker Smart Apex CCD area detector using a graphite monochromated Mo Kα radiation ($\lambda=0.71073$ Å) at 20 °C. The structure was solved by using the program SHELXL and Fourier difference techniques, and refined by full-matrix least-squares method on F^2. All hydrogen atoms were added theoretically. The crystal and experimental data are shown in Table 1.

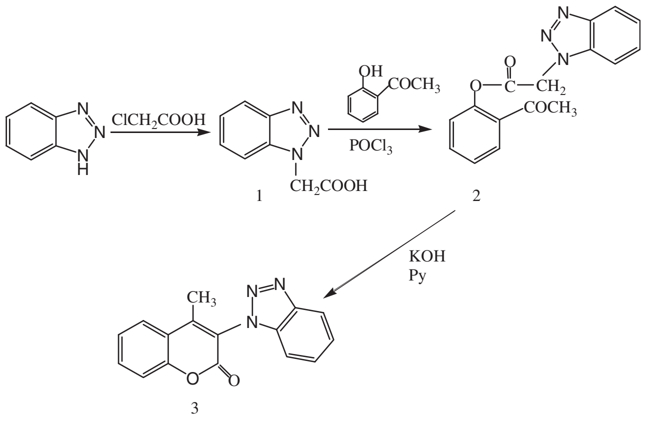

Scheme 1. Synthetic route to the titled compound **3**.

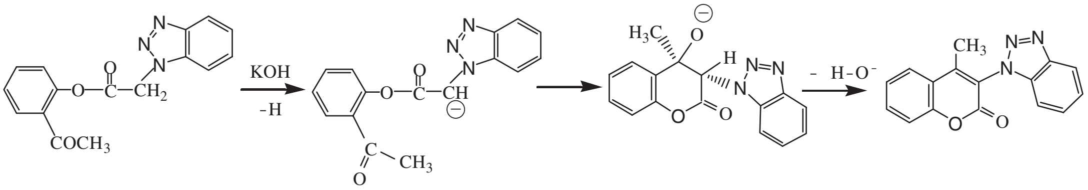

Scheme 2. The mechanism of cyclodehydration.

2.6. Quantum chemical calculations

The structure of BMC was optimized by semiempirical density functional theory (DFT) using a B3LYP/6-31G(d) basis set. The structural energy of BMC was computed at B3LYP/6-31G(d) levels. The structure optimization and energy calculations were performed with the GAUSSIAN 98 program.

3. Results and discussion

3.1. Synthesis

The BMC compound containing electron withdrawing benzotriazole moiety was synthesized by the synthetic route shown in Scheme 1. The first step was alkylation of 1H-benzotriazole with chloroacetic acid in dry toluene. The second step was esterification of (1-benzotriazolyl) acetic acid with 2-hydroxyacetophenone in the presence of phosphorus oxychloride in dry pyridine. The final step was cyclodehydration of (2-acetyl) phenol 2-(1-benzotriazolyl) acetate using potassium hydroxide as catalyst in the dry pyridine.

The mechanism of cyclodehydration is shown in Scheme 2. Bearing electron-withdrawing group, the alkylidene adjacent to benzotriazole easily loses a proton when treated with base and a carbanion forms stably. The carbanion connects to the carbonyl group and the oxy anion attacks the hydrogen intramolecularly. A H-O$^-$ is then eliminated and a new C=C bond is formed.

3.2. X-ray crystallographic analyse

The crystal structure and packing diagram of BMC are given in Fig. 1 and Fig. 2, respectively. The crystal data and experimental details are shown in Table 1. The bond lengths and bond angles of BMC are listed in Table 2.

The single crystal of BMC, suitable for X-ray diffraction analyse, was obtained from methanol solutions and the structure was examined by a single-crystal X-ray diffraction analysis. The crystal of BMC belongs to the orthorhombic space group $Pca2_1$. As shown in Fig. 1, the benzotriazole group is not coplanar with the coumarin ring and the dihedral angle is 108°. This is attributed to steric interaction between 4-positioned methyl group and benzotriazole group. There is an intermolecular π–π stacking between the BMC molecules in crystal lattice as shown in Fig. 2.

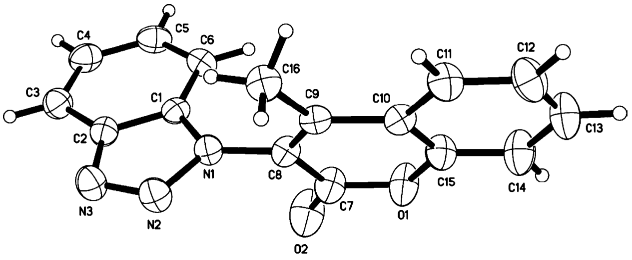

Fig. 1. Crystal structure of BMC.

3.3. Absorption and fluorescence of BMC

UV–vis absorption spectra of BMC and coumarin in diluted chloroform solutions are given in Fig. 3. Two intense absorption bands are observed in the spectra of BMC and coumarin and the spectral shape of BMC is similar to that of coumarin. The absorption spectrum of coumarin has two peaks at 281 and 320 nm, while BMC has two absorption peaks at 275 and 315 nm, respectively. Compared with coumarin, the absorption peaks of BMC shift to blue due to the electron-withdrawing benzotriazole substituent in 3-position. Charge density decreases within the pyranone ring, and thus, there appears a noticeable π-electron density transfer from carbonyl oxygen to pyranone ring. The lower energy absorption maximum of BMC (315 nm) corresponds to $S_0 \rightarrow S_1$ transition.

Fig. 4 shows fluorescence spectra of BMC and coumarin in dilute solutions. It is shown that the emission peaks of BMC and coumarin appeared at around 385 nm and 430 nm, respectively. The emission of BMC was blue-shifted by about 45 nm with respect to that of coumarin because of steric hindrance resulting from benzotriazole and methyl group.

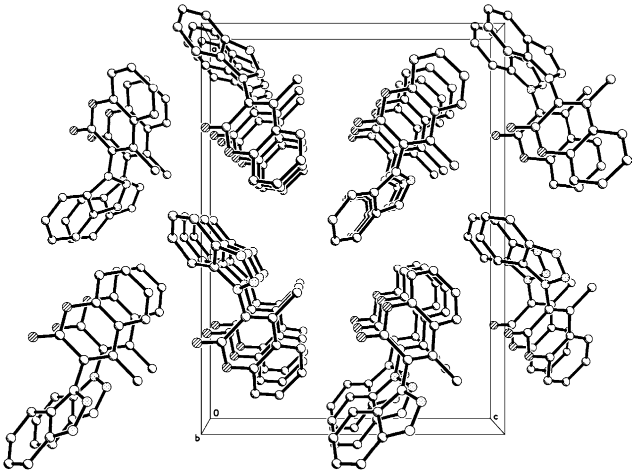

Fig. 2. Packing diagram along *b*-axis. H atoms are omitted for clarity.

Table 2
Experimental and calculated structural parameters of BMC molecule

Bond length (Å)	Exp.	Calcd.	Bond angles (°)	Exp.	Calcd.
O1–C7	1.364(4)	1.3652	C7–O1–C15	121.5(2)	122.8
O1–C15	1.389(4)	1.3815	C1–N1–N2	109.4(2)	109.4612
O2–C7	1.204(4)	1.2082	C1–N1–C8	128.4(2)	130.8264
N1–C1	1.367(4)	1.3747	N2–N1–C8	122.2(2)	119.6938
N1–N2	1.366(3)	1.3887	N3–N2–N1	109.2(2)	109.0601
N1–C8	1.414(4)	1.4136	N2–N3–C2	107.8(2)	109.0178
N2–N3	1.298(4)	1.2845	N1–C1–C2	104.4(3)	103.6797
N3–C2	1.381(4)	1.3814	N1–C1–C6	132.9(3)	134.4108
C1–C2	1.378(4)	1.408	C2–C1–C6	122.6(3)	121.8905
C1–C6	1.405(4)	1.4021	N3–C2–C1	109.2(3)	108.7726
C2–C3	1.399(4)	1.4038	N3–C2–C3	130.6(3)	130.1688
C3–C4	1.364(5)	1.3849	C1–C2–C3	120.3(3)	121.0565
C4–C5	1.394(5)	1.4163	C4–C3–C2	117.6(3)	117.2709
C5–C6	1.362(5)	1.3868	C3–C4–C5	121.2(3)	121.2158
C7–C8	1.445(4)	1.4712	C6–C5–C4	122.9(3)	122.1957
C8–C9	1.349(4)	1.3671	C5–C6–C1	115.4(3)	116.3701
C9–C10	1.451(4)	1.4554	O2–C7–O1	117.3(3)	118.222
C9–C16	1.483(4)	1.5045	O2–C7–C8	125.6(3)	125.6812
C10–C15	1.377(4)	1.4068	O1–C7–C8	117.1(3)	116.085
C10–C11	1.400(5)	1.4106	C9–C8–N1	122.0(3)	121.9677
C11–C12	1.369(4)	1.3877	C9–C8–C7	123.5(3)	122.8209
C12–C13	1.379(5)	1.4021	N1–C8–C7	114.5(3)	115.1706
C13–C14	1.373(5)	1.3894	C8–C9–C10	117.2(3)	117.9934
C14–C15	1.379(4)	1.3956	C8–C9–C16	122.2(3)	122.8028
			C10–C9–C16	120.6(3)	119.2038
			C15–C10–C11	116.7(3)	117.4891
			C15–C10–C9	119.6(3)	118.7218
			C11–C10–C9	123.6(3)	123.7887
			C12–C11–C10	120.9(3)	121.0271
			C11–C12–C13	120.5(3)	120.0709
			C14–C13–C12	120.2(3)	120.2927
			C13–C14–C15	118.4(3)	119.1197
			C10–C15–O1	121.1(2)	121.4714
			C10–C15–C14	123.3(3)	122.0002
			O1–C15–C14	115.6(3)	116.528

3.4. Quantum chemical calculations

The total energy of BMC obtained at B3LYP/6-31G(d) level of theory was −930.7834098 (au). The B3LYP/6-31G(d)-optimized structure of BMC is shown in Fig. 5, indicating that the DFT-optimized structure is close to the crystal structure. Atomic charges of hetero atoms and dipole moment of BMC molecule are listed in Table 3.

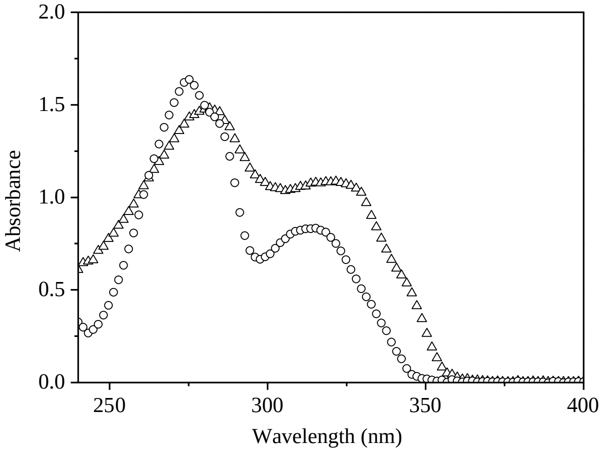

Fig. 3. UV-vis absorption spectra of BMC (○) and coumarin (Δ) in chloroform (2×10^{-5}mol/l).

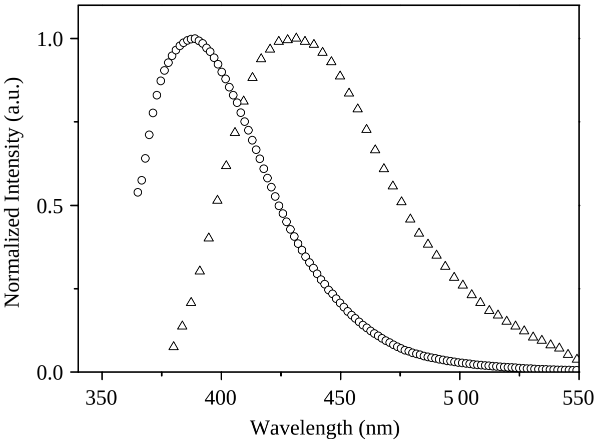

Fig. 4. Fluorescence spectra of BMC (○) and coumarin (Δ) in dilute chloroform solutions at room temperature. ($C=2\times10^{-5}$ mol/l, $\lambda_{ex}=360$ nm.)

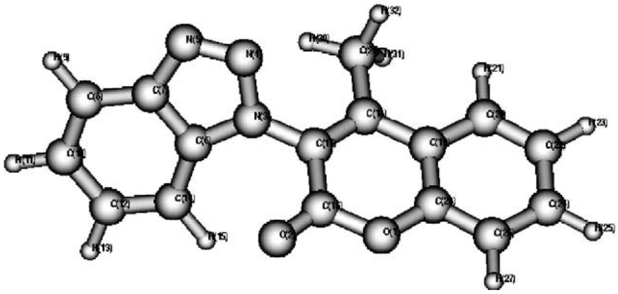

Fig. 5. B3LYP/6-31G(d)-optimized structure of BMC.

B3LYP/6-31G(d)-optimized geometrical data of BMC were obtained. It was found that the B3LYP/6-31G(d) optimized structure of BMC is in good agreement with the X-ray crystallographic data as listed in Table 2. Therefore, the results using density functional theory (DFT) at B3LYP/6-31G(d) level is creditable. The HOMO and LUMO levels of BMC were deduced using the DFT method as shown in Fig. 6, which is essential for deducing its S_0 and S_1 states. This knowledge is important for the better understanding of its fluorescence and nonlinear optical properties.

Table 3
Atomic charges of hetero atoms and dipole moment of BMC

Atom	Mulliken[a]
O(1)	−0.518559
O(2)	−0.456091
N(3)	−0.498957
N(4)	−0.053297
N(5)	−0.367091
Dipole moment, *D*	7.0130

[a] In hartree based on the B3LYP/6-31G(d) level.

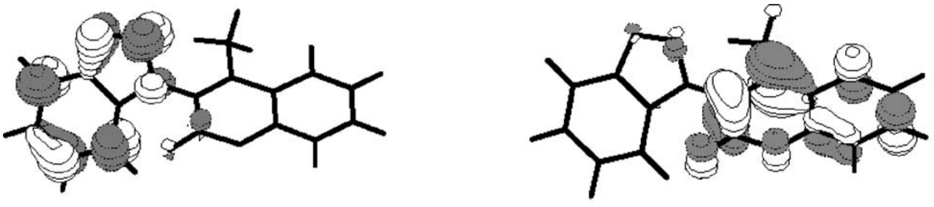

LUMO+1 (–1.0358 eV) LUMO (–2.1096 eV)

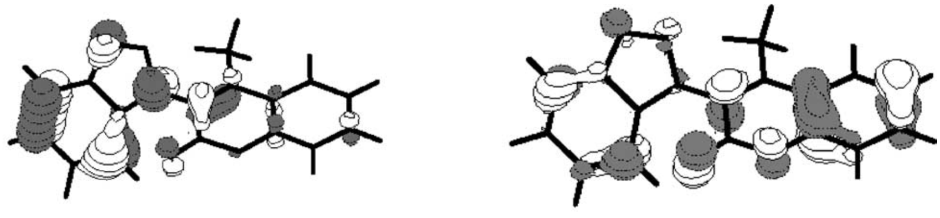

HOMO (–6.3817 eV) HOMO-1 (–6.7937 eV)

Fig. 6. Frontier molecular orbitals of compound BMC.

From Fig. 6, it can be seen that the HOMO of BMC is −6.38 eV and the LUMO is −2.11 eV. The electron density of the HOMO is localized mostly on the benzotriazole ring, and inversely, the LUMO is localized mainly on the coumarin ring. The presence of electron-withdrawing benzotriazole at 3-position has a large effect on frontier orbitals, and thus the LUMO of BMC is higher than that of coumarin [10].

Further investigation on the electroluminescent properties of BMC is being carried out.

4. Conclusions

The novel coumarin derivative, BMC, containing an electron-transporting moiety was synthesized, and the reaction mechanism was also discussed. Its structure was studied both experimentally and theoretically. Both the absorption and emission spectra of BMC were blue-shifted with respect to those of coumarin because of the electron-withdrawing substitute and steric hindrance. The HOMO and LUMO levels of BMC were deduced and the LUMO energy of BMC was elevated by introducing the electron-withdrawing moiety.

5. Supplementary material

The crystallographic data (excluding structure factors) of BMC has been deposited with the Cambridge Crystallographic Center as supplementary publication no. CCDC-286841.

Acknowledgements

This work was supported by ‘Qing Lan’ talent engineering funds (QL-06-01A) of the Lanzhou Jiaotong University.

References

[1] R. O’Kennedy, in: R.D. Thornes (Ed.), Coumarins. Biology, Applications and Mode of Action, Wiley, Chichester, 1997.
[2] K.H. Drexhage, in: F.P. Schäfer (Ed.), Topics in Applied Physics Dye Lasers, vol. 1, Springer, Berlin, 1973.
[3] G. Jones, W.R. Jackson, C. Choi, W.R. Bergmark, J. Phys. Chem. 89 (1985) 294.
[4] T. Hiroshi, O. Yosho, I. Juzo, I. Masato, T. Atsushi, Jpn. Kokai Tokkyo Koho, 1990 (1990) (CODEN JKXXAF JP 02126241 A2 19900515 Heisei).
[5] H.E. Patel, K.R. Desai, J. Inst. Chem. 68 (1996) 78.
[6] R.P. Haugland, Handbook of Fluorescent Probes and Research Chemicals, Molecular Probes, Eugene (OR), 1994–1996.
[7] H. Schwander, P. Hendrix, in: Y.S. Yamamoto (Ed.), fifth ed. Ullmann’s encyclopedia of industrial chemistry, vol. A11, VCH, Weinheim, 1988, p. 280.
[8] H.K. Arora, A.R. Aggarwal, P. Singh, Indian J. Chem. 21A (1982) 844.
[9] O.S. Wolfbeis, E. Koller, P. Hochmuth, Bull. Chem. Soc. Jpn 58 (1985) 731.
[10] I. Novak, B. Kovač, J. Electron. Spectrosc. 113 (2000) 9.
[11] B.M. Krasovitskii, in: B.M. Krasovitskii, B.M. Bolotin (Eds.), Organic Luminescent Materials, VCH, Weinheim, 1988 (Chapter 7).
[12] F. Gao, H.-R. Li, Y.-Y. Yang, Dyes Pigm. 47 (2000) 231.
[13] B. Bangar Raju, B. Eliasson, J. Photochem. Photobiol. A: Chem. 116 (1998) 135.
[14] C.W. Tang, S.A. VanSlyke, C.H. Chen, J. Appl. Phys. 65 (1989) 3610.
[15] J. Kido, K. Hongawa, K. Okuyama, K. Nagai, Appl. Phys. Lett. 64 (1994) 815.
[16] C.C. Wu, J.C. Sturm, R.A. Register, J. Tian, E.P. Dana, M.E. Thompson, IEEE Tans. Electron Devices 44 (1997) 1269.
[17] T. Mori, K. Obata, K. Imaizumi, T. Mizutani, Appl. Phys. Lett. 69 (1996) 3309.
[18] Y. Hamada, H. Kanno, T. Sano, H. Fujii, Y. Nishio, H. Takahashi, T. Usuki, K. Shibata, Appl. Phys. Lett. 72 (1998) 1939.
[19] H.P. Zheng, R.F. Zhang, F. Wu, W.J. Tian, J.C. Shen, Synth. Met. 100 (1999) 291–295.
[20] S.A. Swanson, G.M. Wallraff, J.P. Chen, W.J. Zhang, L.D. Bozano, K.R. Carter, J.R. Salem, R. Villa, J.C. Scott, Chem. Mater. 15 (2003) 2305.
[21] S.H. Ahn, M. Czae, E.R. Kim, H. Lee, S.H. Han, J. Noh, M. Hara, Macromolecules 34 (2001) 2522.
[22] J.T. Gupton, F.A. Hicks, S.Q. Smith, A.D. Main, S.A. Petrich, D.R. Wilkinson, J.A. Sikorski, A.R. Katritzky, Tetrahedron 49 (1993) 10205.
[23] F.M. Liu, Z.F. Zhang, Y.T. Liu, S.X. Kong, Y.Z. Chen, Chin. J. Org. Chem. 20 (2000) 499.